Inorganica Chimica Acta 363 (2010) 2215–2221

Contents lists available at ScienceDirect

Inorganica Chimica Acta

journal homepage: www.elsevier.com/locate/ica

Synthesis, characterization and anti-diabetic effect of *bis*[(1-*R*-imidazolinyl)phenolato]oxovanadium(IV) complexes

Ryan S. Walmsley [a], Zenixole R. Tshentu [a,*], Manuel A. Fernandes [b], Carminita L. Frost [c]

[a] Department of Chemistry, Rhodes University, P.O. Box 94, Grahamstown 6140, South Africa
[b] Molecular Sciences Institute, School of Chemistry, University of Witwatersrand, P.O. Wits 2050, Johannesburg, South Africa
[c] Department of Biochemistry and Microbiology, Nelson Mandela Metropolitan University, P.O. Box 77000, Port Elizabeth 6031, South Africa

ARTICLE INFO

Article history:
Received 2 December 2009
Received in revised form 8 March 2010
Accepted 11 March 2010
Available online 16 March 2010

Keywords:
Oxovanadium
Imidazoline
Glucose uptake

ABSTRACT

The five-coordinate oxovanadium(IV) complexes; $[VO(pimin)_2]$ (**1a**), $[VO(Etpimin)_2]$ (**2**) and $[VO(EtOHpimin)_2]$ (**3**), were prepared by reacting the ligands; 2-(2′-hydroxyphenyl)-1*H*-imidazoline (piminH), 2-(2′-hydroxyphenyl)-1-ethylimidazoline (EtpiminH) and 2-(2′-hydroxyphenyl)-1-ethanolimidazoline (EtOHpiminH), with $VOSO_4$. The complexes were characterized by elemental analysis, IR, UV–Vis and cyclic voltammetry. All complexes show V=O stretching vibrations between 932 and 987 cm^{-1}. The presence of three d–d transition occurring between 400 and 625 nm and the irreversible oxidation ($V^{IV} \rightarrow V^{V}$) between 400 and 490 mV confirm the d^1 electronic configuration of the complexes. The solid state structures of $[VO(pimin)_2]$ (**1a**) and its autoxidation hydrolysis product $[VO_2(pimin)(piminH')]$ (**1b**) were determined by single crystal X-ray diffraction. The geometry of $[VO(pimin)_2]$ was found to be intermediate between trigonal bipyramidal and square pyramidal and sits on a crystallographic twofold axis, while the geometry of $[VO_2(pimin)(piminH')]$ was distorted trigonal bipyramidal. Potentiometric titrations were used to determine the protonation and stability constants for the ligands and oxovanadium(IV) complexes, respectively. The species existing over a biological pH range were also investigated. The *in vitro* studies indicated that the oxovanadium(IV) complexes were effective in enhancing glucose uptake in the 3T3-L1 adipocytes, C2C12 muscle cells and Chang liver cell lines. In these cell lines, the anti-hyperglycemic effect was equivalent to or surpassed the effect of metformin.

© 2010 Elsevier B.V. All rights reserved.

1. Introduction

Diabetes mellitus has become a growing health concern with approximately 180 million people currently affected by the disease worldwide [1]. Almost 80% of the deaths associated with diabetes occur in low and middle-income countries [2], and the total number of those afflicted is set to double by 2030 [3]. The ever increasing prevalence of diabetes has driven the development of pharmaceuticals that do not exhibit the undesirable side-effects of current therapies, and vanadium has shown promise in this regard [4,5]. Inorganic salts of vanadium have shown significant insulin-enhancing effects [6,7] but the potential toxicity of vanadate and low absorption rate of vanadyl sulfate [8,9] has pushed the focus towards designing new organovanadium compounds. Tailoring of the properties of these vanadium complexes can thus be achieved by simple modification of the organic ligand.

The ligands stabilize vanadium under the pH conditions of the digestive tract and assist absorption of vanadium into the blood stream, where the vanadium complexes may experience ligand substitution as well as undergo redox reactions ($V^{IV} \rightleftharpoons V^{V}$) [10,11]. Vanadium may then be shuttled by bio-ligands to the cell which it enters via diffusion, endocytosis or ion-channels (in the form of vanadate) [12].

Vanadate is structurally similar to phosphate and is thus able to bind and inhibit protein tyrosine phosphatase (PTP), an enzyme which counteracts the autophosphorylation effects of insulin. As a result, the insulin-induced signal transduction pathway remains intact and the metabolism of glucose is improved [12]. The most illustrious of these glucose-lowering organovanadium compounds include *bis*(picolinato)oxovanadium(IV) [13], *bis*(maltolato)oxovanadium(IV) (BMOV), and *bis*(ethylmaltolato)oxovanadium(IV) (BEOV), with the latter having undergone Phase IIa clinical trials [14].

In this paper, we present the synthesis and characterization of three novel oxovanadium(IV) compounds with 2-(2′-hydroxyphenyl)-1*R*-imidazoline ligands. The stability and pH speciation of the complexes, as well as their *in vitro* glucose-lowering effect, was investigated. Certain imidazoline compounds have been shown to have anti-diabetic effect [15,16], hence we have chosen this group as a binding moiety to oxovanadium(IV).

* Corresponding author. Tel.: +27 46603 8846; fax: +27 46622 5109.
E-mail address: z.tshentu@ru.ac.za (Z.R. Tshentu).

0020-1693/$ - see front matter © 2010 Elsevier B.V. All rights reserved.
doi:10.1016/j.ica.2010.03.028

2. Experimental

2.1. Materials, methods and instrumentation

All chemicals were purchased from commercial sources (Sigma–Aldrich, Merck) and used without further purification. Solvents were of reagent grade. All oxovanadium(IV) complexes were synthesized under an argon atmosphere.

The infrared spectra were recorded on a Perkin Elmer 2000 FTIR spectrometer in the mid-IR range (4000–400 cm^{-1}) as KBr pellets. ^1H and ^{13}C NMR spectra of all ligands were recorded on a Bruker AMX 400 NMR MHz spectrometer and reported relative to tetramethylsilane (δ 0.00). Electronic spectra were recorded on a Varian Cary 500 Scan UV–Vis spectrophotometer using 1 cm quartz cells and dimethylsulfoxide as the solvent. Microanalysis was carried out using a Vario Elementar Microcube ELIII. Cyclic voltammetry was performed using a BAS CV 100 Cyclic Voltammogram. Potentiometric studies were performed using a Metrohm 794 Titrino equipped with a Metrohm LL Ecotrode. A Bio-Tek KC4 powerwave XS microtiter plate reader was used to measure absorbance for 3-(4,5-dimethylthiazol-2-yl)-2,5-diphenyl tetrazolium bromide (MTT) and Glucose assays.

2.2. Preparative work

2.2.1. 2-(2′-Hydroxyphenyl)-1H-imidazoline (piminH)

Methyl salicylate (1.84 g, 0.012 mol) was added to an excess of ethylenediamine (3.2 g, 0.053 mol) in a conical flask and heated in a microwave for 7 min at 180 W. Excess ethylenediamine was distilled off under reduced pressure until a solid material was left behind. This solid was then digested overnight in chloroform, filtered and then washed with cold chloroform to afford a cream solid. Yield: 78.1%. ^1H NMR (400 MHz, DMSO-d_6): δ 3.71 (s, 4H, Im–CH_2), 6.69 (t, 1H, Ar–H) 6.77 (d, 1H, Ar–H), 7.27 (t, 1H, Ar–H), 7.56 (d, 1H, Ar–H). ^{13}C NMR (400 MHz, DMSO-d_6): δ 46.5, 110.2, 115.5, 118.4, 127.2, 132.7, 163.5, 166.1; IR (cm^{-1}, KBr disk): 3217, ν(N–H); 1618, ν(C=N). *Anal.* Calc. for $C_9H_{10}N_2O$: C, 66.65; H, 6.21; N, 17.27. Found: C, 66.68; H, 6.20; N, 16.98%.

2.2.2. 2-(2′-Hydroxyphenyl)-1-ethylimidazoline (EtpiminH)

This was prepared in a similar manner as above except that *N*-ethylethylenediamine was used. Yield: 50.3%. ^1H NMR (δ, 400 MHz, $CDCl_3$): 1.26 (t, 3H, N–CH_2CH_3), 3.42 (q, 2H, N–CH_2), 3.50 (t, 2H, Im–CH_2), 3.91 (t, 2H, Im–CH_2), 6.76 (t, 1H, Ar–H), 6.98 (d, 1H, Ar–H), 7.27 (t, 1H, Ar–H), 7.36 (t, 1H, Ar–H). ^{13}C NMR (δ, 400 MHz, $CDCl_3$): 14.50, 45.52, 50.47, 50.92, 112.31, 117.11, 118.66, 127.31, 132.16, 162.19, 167.09. IR (cm^{-1}, KBr disk): 1608, ν(C=N); *Anal.* Calc. for $C_{11}H_{14}N_2O$: C, 69.45; H, 7.42; N, 14.73. Found: C, 69.54; H, 7.67; N, 14.44%.

2.2.3. 2-(2′-Hydroxyphenyl)-1-ethanolimidazoline (EtOHpiminH)

This was prepared in a similar manner as for piminH above except that *N*-ethanolethylenediamine was used. Yield: 54.1%. ^1H NMR (δ, 400 MHz, D_2O): 3.57 (t, 2H, N–CH_2), 3.79 (t, 2H, N–CH_2CH_2), 4.11 (m, 4H, Im–CH_2), 6.70 (t, 1H, Ar–H), 6.76 (d, 1H, Ar–H), 7.27 (d, 1H, Ar–H), 7.43 (t, 1H, Ar–H). ^{13}C NMR (δ, 400 MHz, D_2O): 43.13, 49.15, 49.19, 58.18, 112.21, 114.18, 121.81, 130.19, 134.93, 166.02, 169.49. IR (cm^{-1}, KBr disk): 3138 ν(O–H); 1612, ν(C=N). *Anal.* Calc. for $C_{11}H_{14}N_2O_2$: C, 64.06; H, 6.84; N, 13.58. Found: C, 64.31; H, 6.55; N, 13.44%.

2.2.4. [VO(pimin)$_2$] (**1a**)

To a solution of Hpimin (0.25 g, 1.5 mmol) in methanol (5 ml) was added vanadyl sulfate (0.152 g, 0.70 mmol) in water (5 ml). A blue–green precipitate formed immediately. The reaction was allowed to proceed for a further 2 h. The precipitate was collected, washed with water, then methanol and dried at 100 °C. Yield: 56.9%. IR (cm^{-1}, KBr disk): 931, ν(V=O); 3260, ν(N–H); 1609, ν(C=N). *Anal.* Calc. for $C_{18}H_{18}N_4O_3V$: C, 55.53; H, 4.66; N, 14.39. Found: C, 55.43; H, 4.74; N, 14.16%. UV–Vis (DMSO) λ_{max} (ε, M^{-1} cm^{-1}): 617 (55), 542 (44), 403sh (196).

Upon standing the synthetic mother liquor at room temperature and under aerobic conditions, yellow crystals of [VO_2(pimin)(piminH′)] (**1b**) were obtained. Yield wrt V: 12.3%. IR (cm^{-1}, KBr disk): 931, 886, ν(V=O); 3191, ν(N–H); 1617, ν(C=N). *Anal.* Calc. for $C_{18}H_{19}N_4O_4V$: C, 53.21; H, 4.71; N, 13.79. Found: C, 53.14; H, 4.71; N, 13.82%.

2.2.5. [VO(Etpimin)$_2$] (**2**)

This was prepared in a similar manner as above except that EtpiminH was used. Yield: 47.6%. IR (cm^{-1}, KBr disk): 987, ν(V=O); 1602, ν(C=N). *Anal.* Calc. for $C_{22}H_{26}N_4O_3V$: C, 59.32; H, 5.88; N, 12.58. Found: C, 59.04; H, 5.88; N, 12.27%. UV–Vis (DMSO) λ_{max} (ε, M^{-1} cm^{-1}): 621 (120), 547 (99), 401sh (300).

2.2.6. [VO(EtOHpimin)$_2$] (**3**)

This was prepared in a similar manner as for **1a** except that EtOHpiminH was used. Yield: 52%. IR (cm^{-1}, KBr disk): 966, ν(V=O); 1603, ν(C=N). *Anal.* Calc. for $C_{22}H_{26}N_4O_5V$: C, 55.35; H, 5.49; N, 11.74. Found: C, 55.30; H, 5.63; N, 11.66%. UV–Vis (DMSO) λ_{max} (ε, M^{-1} cm^{-1}): 625 (84), 548 (66), 404sh (269).

2.3. Cyclic voltammetry

Cyclic voltammograms of **1a**, **2** and **3** were recorded using a glassy carbon electrode as the working electrode, platinum wire as the counter electrode and silver chloride-coated silver wire as the reference electrode. For all complexes, DMSO was used as the solvent and tetrabutylammonium perchlorate was used as the supporting electrolyte. Argon was bubbled through the solutions for 5 min before each run. A scan rate of 100 mV s^{-1} was used.

2.4. Potentiometric studies

The protonation and stability constants for the ligands and oxovanadium(IV) complexes were determined by potentiometric titration of approximately 25 ml samples. All solutions were prepared using freshly boiled and degassed deionized milli-Q water to ensure the removal of dissolved oxygen and carbon dioxide. The ligand concentration was 1 mM and metal-to-ligand ratios of 1:1, 1:5 and 1:10 were used. Titrations were performed over the pH range of 2–11 under a continuous flow of purified nitrogen using HCl and tetramethylammonium hydroxide (TMAOH). The vanadium stock solution containing 0.10 M HCl was standardized by titration with permanganate. The ionic strength of the titration solutions was kept constant at 0.10 M tetramethylammonium chloride (TMACl). Titrations were controlled using Tiamo software. The glass electrode was calibrated for a strong acid–base reaction by the Gran-method [17] using the program GLEE [18], to determine the standard potential E^o. The ionic product of water (pK_w) of 13.83(1) at 25.0 ± 0.1 °C in 0.10 M TMACl was used in all calculations [19]. The hydrolysis model of a vanadyl system was included in the model; $[VO(OH)]^+$ ($\log \beta_{10-1} = -5.94$) and $[(VO)_2(OH)_2]^{2+}$ ($\log \beta_{20-2} = -6.95$), while $[VO(OH)_3]^-$ ($\log \beta_{10-3} = -18.0$) and $[(VO)_2(OH)_5]^-$ ($\log \beta_{20-5} = -22.0$) [20] did not fit. The concentration stability constants $\beta_{pqr} = [M_pL_qH_r]/[M]^p[L]^q[H]^r$ were calculated by using the computer program HYPERQUAD [21]. The final values of the constants were obtained from an average of six independent titrations using an average of 400 data points in total for each refinement.

2.5. X-ray crystal structure resolution and refinement

Intensity data for **1a** and **1b** were collected on a Bruker APEX II CCD area detector diffractometer with graphite monochromated Mo Kα radiation (50 kV, 30 mA) using the APEX 2 data collection software [22]. The collection method involved ω-scans of width 0.5° and 512 × 512 bit data frames. Data reduction was carried out using the program SAINT+ [23] and absorption corrections were made using the program SADABS [23].

The crystal structures were solved by direct methods using SHELXTL [24]. Non-hydrogen atoms were first refined isotropically followed by anisotropic refinement by full matrix least-squares calculations based on F^2 using SHELXTL. Hydrogen atoms were first located in the difference map then positioned geometrically and allowed to ride on their respective parent atoms. Diagrams and publication material were generated using SHELXTL, PLATON [25] and ORTEP-3 [26].

2.6. In vitro studies

2.6.1. Maintenance of cells lines

3T3-L1 preadipocytes, were maintained in Dulbecco's modified eagle medium (DMEM) supplemented with 10% fetal bovine serum (FBS), while C2C12 mouse skeletal myoblasts and Chang liver cells were maintained in RPMI-1640 medium (Sigma) supplemented with 10% FBS. These were incubated at 37 °C in a humidified incubator with 5% CO_2. Cells were subcultured at 70% confluence and seeded at a density of 35 000 cells/ml (for 3T3-L1) and 25 000 cells/ml (for Chang and C2C12) in 24-well culture plates.

2.6.2. MTT cytotoxicity studies

Cells were seeded in 24-well plates (Nunc) at densities of 25 000 for C2C12 and Chang liver cells, and 35 000 cells/mL for 3T3-L1. After overnight attachment, the culture medium was replaced with medium containing the test compounds at a range of concentrations (0.5–100 μM). Cells were incubated for 48 h at 37 °C, after which the MTT assay was performed [27].

2.6.3. Glucose uptake studies

The glucose uptake assay was performed using the GLUCOSE (Glu-cinet) kit (BAUER) [28]. Control cells (Con) were represented by untreated differentiated fat (3T3-L1), liver (Chang) and muscle (C2C12) cells incubated in culture media. Positive control cells (Met) were represented by untreated differentiated fat, liver and muscle cells exposed to metformin. Cells were then exposed for 48 h to the test compounds. Thereafter glucose uptake was determined and the cell number was normalized using the MTT assay, as laid out by Mossman [27].

2.6.4. Statistical analysis

Error bars indicate the standard error of the mean (SEM) unless specified otherwise ($n = 3$). The two-tail paired test was used to determine significance of results ($p < 0.05$) and ($p < 0.01$).

3. Results and discussion

3.1. Synthesis and general considerations

The ligands were synthesized according to a method by Parík et al. [29] with modifications by us. The ligand 2-(2′-hydroxyphenyl)-*1H*-imidazoline was substituted with the R-groups (R = Et, EtOH) with the goal of balancing the lipophilicity/hydrophilicity, a requirement of these metallopharmaceuticals [30]. The complexes were synthesized by addition of an aqueous vanadyl sulfate solution to a methanolic solution of the corresponding ligand in a 1:2 M ratio (Scheme 1). The complexes which precipitated out of solution were easily collected by filtration.

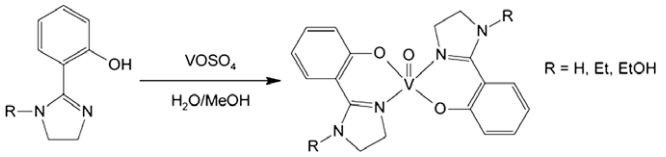

Scheme 1. Synthesis of *bis*[(imidazolinzyl)phenolato]oxovanadium(IV) complexes.

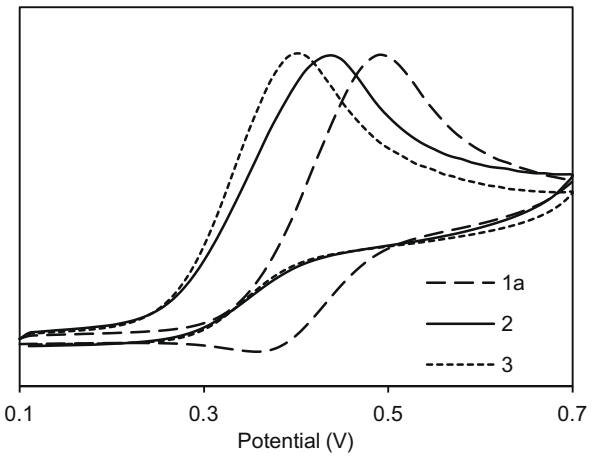

Fig. 1. Cyclic voltammograms of complexes [VO(pimin)$_2$] (**1a**), (E_{pa} = 490 mV); [VO(Etpimin)$_2$] (**2**), (E_{pa} = 440 mV); and [VO(EtOHpimin)$_2$] (**3**), (E_{pa} = 400 mV); in DMSO.

Complexes **1a**, **2** and **3** were soluble in alcohols, DMF and DMSO. Complexes **2** and **3** were also soluble in dichloromethane, acetonitrile and slightly soluble in water. The hydrolysis of these complexes accompanied by autoxidation occurred when the mother liquor was left to stand at room temperature. This was noted by the change in color of the solution from green (V^{IV}) to yellow–green (a mixture of V^{IV} and V^{V}). From the mother liquor of **1a**, yellow crystals deposited from the yellow–green solution. This oxidation product was identified as the dioxovanadium(V) species, **1b**.

The low oxidation potential of the complexes, determined by cyclic voltammetry, corresponds well with the facile aerobic oxidation observed in solution. All complexes display irreversible V^{IV}–V^{V} oxidation peaks between 400 and 490 mV (Fig. 1).

3.2. Spectroscopic characterization

All of the ligands display infrared stretching frequencies between 1618 and 1608 cm^{-1} which can be assigned to the azomethine (C=N) stretch [29]. Coordination to oxovanadium(IV) was evident from a ~9 cm^{-1} shift of this stretch to lower frequencies [31]. The uncoordinated ligands show phenolic ν(C–O) stretches between 1287 and 1269 cm^{-1} which upon coordination shift to a higher wavelength of 1313–1319 cm^{-1} [32]. The ν(V=O) bands appear at 932, 987 and 965 cm^{-1} for **1a**, **2** and **3**, respectively, and are within the reported range for V=O stretches of 930–1030 cm^{-1} [33]. For the dioxovanadium(V) complex **1b**, two ν(V=O) bands appear at 931 and 886 cm^{-1}. The higher energy band is assigned to the ν_{as} stretch and the lower energy band is assigned to the ν_s stretch of the *cis*-VO_2^+ moiety [34].

In general, square pyramidal oxovanadium(IV) complexes display three low intensity d–d transitions in the range of 330–1000 nm [35]. The high energy transition, $b_2 \rightarrow a_1$, occurs between

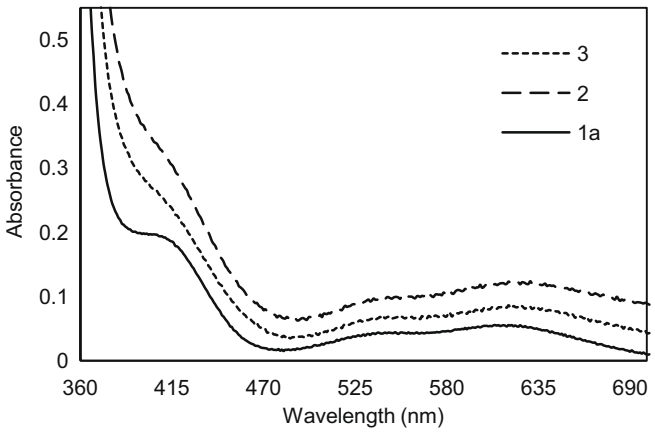

Fig. 2. Electronic spectra of [VO(pimin)$_2$] (**1a**), [VO(Etpimin)$_2$] (**2**) and [VO(EtOHpimin)$_2$] (**3**).

401 and 404 cm^{-1} as a shoulder to a charge transfer band, hence the higher intensity. The $b_2 \rightarrow b_1$ and $b_2 \rightarrow e$ transitions fall in the range 538–545 cm^{-1} and 617–625 cm^{-1}, respectively (Fig. 2).

3.3. X-ray crystallography

The blue–green crystals of **1a** suitable for X-ray crystallography were obtained upon recrystallization of the compound in acetonitrile at −20 °C. The yellow crystals of **1b** were obtained from standing a methanolic mother liquor of **1a** at room temperature for 4 days. The ORTEP diagrams for the structures of **1a** and **1b** are represented by Figs. 3 and 4, respectively. The selected crystallographic data is presented in Table 1 and selected bond lengths and angles in Table 2. For **1a**, the V=O bond length of 1.619(2) Å is slightly longer than those observed for similar compounds, which fall in the range of 1.591–1.605 Å [36,37]. The geometry of **1a** is intermediate between trigonal bipyramidal and square pyramidal with τ = 0.49 [38] and sits on a crystallographic twofold axis. Vanadium is situated 0.550 Å above the plane defined by the N_2O_2 ligand donor atoms and the N(1)–V(1)–O(2) and O(1)–V(1)–O(2) angles are 99.12(6)° and 113.92(6)°, respectively. The N(1)–V(1)–N(1) and O(1)–V(1)–O(1) angles in the equatorial plane are 161.8(1)° and 132.2(1)°, respectively, showing marked deviations from an ideal of 180° expected for a square pyramidal geometry.

The bidentate ligand coordinates through the neutral imidazoline nitrogen and phenolate oxygen resulting in the formation of the neutral *bis*[(imidazolinyl)phenolato]oxovanadium(IV) complex. The average bite angle of the ligands is 86.32(8)°. The V(1)–O(1) and V(1)–N(1) bond lengths have averages of 1.911(1) and 2.048(2) Å, respectively. The imidazoline and phenyl rings are not co-planar, and have an average dihedral angle of 20.11° between them. As expected, the imidazoline ring is not planar with the torsion angles C(9)–C(8)–N(1)–C(7) = 13.4(3)° and C(8)–C(9)–N(2)–C(7) = 16.9(3)°.

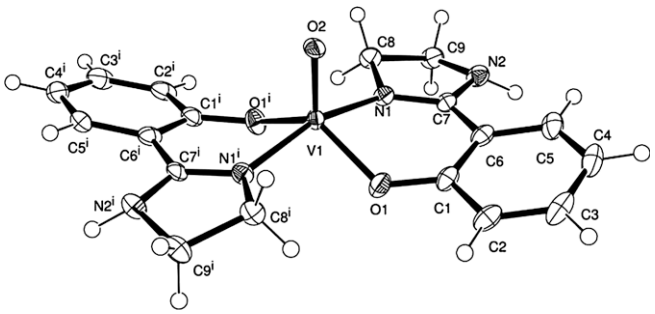

Fig. 3. ORTEP diagram of **1a**, showing 50% thermal probability ellipsoids.

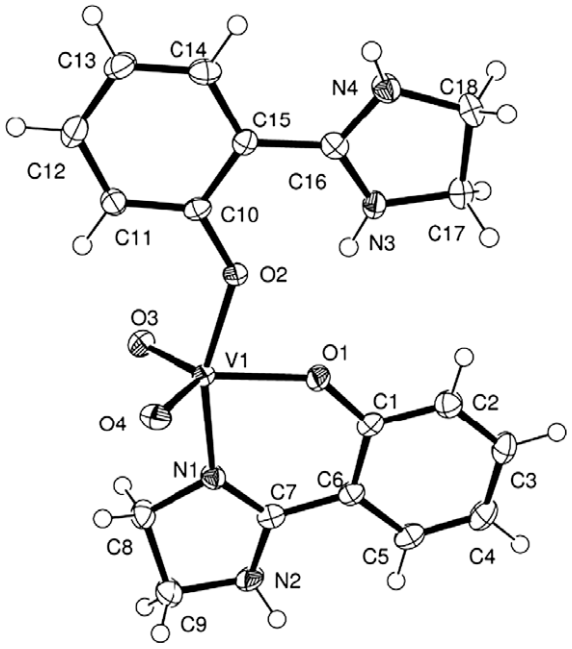

Fig. 4. ORTEP diagram of **1b**, showing 50% thermal probability ellipsoids.

Table 1
Selected crystallographic data for [VO(pimin)$_2$] (**1a**) and [VO$_2$(pimin)(piminH′)] (**1b**).

Compound	[VO(pimin)$_2$] (**1a**)	[VO$_2$(pimin)(piminH′)] (**1b**)
Empirical formula	$C_{18}H_{18}N_4O_3V$	$C_{18}H_{19}N_4O_4V$
Formula weight	389.30	406.32
Crystal color	blue–green	yellow
Crystal system	orthorhombic	monoclinic
Space group	*Fdd2*	$P2_1/c$
Temperature (K)	173(2)	173(2)
a (Å)	12.4698(7)	8.9544(8)
b (Å)	36.810(2)	22.6383(19)
c (Å)	7.3123(4)	8.6648(7)
α (°)	90	90
β (°)	90	90.736(2)
γ (°)	90	90
V (Å^3)	3356.5(3)	1756.3(3)
Z	8	4
ρ_{calc} (g/cm^3)	1.541	1.537
Wavelength (Å)	0.71073	0.71073
Total reflections	4875	12 519
Unique reflections	1827	4234
R	0.0384	0.0501
R_w	0.0735	0.0962

Table 2
Selected bond lengths (Å) and angles (°) for [VO(pimin)$_2$] (**1a**) and [VO$_2$(pimin)(piminH′)] (**1b**).

[VO(pimin)$_2$] (**1a**)		[VO$_2$(pimin)(piminH′)] (**1b**)	
V(1)–O(2)	1.619(2)	V(1)–O(3)	1.617(1)
V(1)–O(1)	1.911(1)	V(1)–O(4)	1.648(1)
V(1)–N(1)	2.048(2)	V(1)–O(1)	1.949(1)
O(1)–V(1)–O(1)	132.2(1)	V(1)–O(2)	1.932(1)
N(1)–V(1)–N(1)	161.8(1)	V(1)–N(1)	2.062(2)
O(1)–V(1)–O(2)	113.91(6)	O(3)–V(1)–O(4)	108.3(1)
N(1)–V(1)–O(2)	99.12(6)	O(1)–V(1)–O(3)	128.08(9)
N(1)–V(1)–O(1)	86.26(8)	O(1)–V(1)–O(4)	123.40(9)
N(1)–V(1)–O(1)^i	86.37(8)	N(1)–V(1)–O(2)	159.07(8)

The five-coordinate dioxovanadium(V) complex, [VO_2(pimin)-(piminH′)] (**1b**), adopts a highly distorted trigonal bipyramidal geometry (τ = 0.59) with O(1), O(3) and O(4) forming the trigonal plane. The deviations in this plane are given by O(1)–V(1)–O(3) = 128.05(9)°, O(1)–V(1)–O(4) = 123.40(9)° and O(3)–V(1)–O(4) = 108.3(1)°. The N(1)–V(1)–O(2) at 159.02(8)° is also far from the ideal of 180°.

The V(1)–O(3) and V(1)–O(4) at 1.617(1) and 1.648(1) Å, respectively, are within the lengths expected for a five-coordinate dioxovanadium(V) systems [34]. However, the V(1)–O(4) length is slightly longer due to strong hydrogen bonding with N(2)–H of the neighboring molecule [N(2)–H···O(4) = 2.00(2) Å]. One of the ligands attaches to the dioxovanadium(V) center in a monodentate fashion through the phenolate oxygen while the other ligand attaches in a bidentate manner through the imidazoline nitrogen (N1) and phenolate oxygen (O1) with a bite angle of 81.56(8)°. The imidazoline nitrogen (N3) of the mono-coordinated ligand is protonated to afford a positively charged species which neutralizes the extra negative charge resulting from the two phenolate oxygens and the two dioxo ligands, and the vanadium(V) center.

3.4. pH speciation

The protonation constants of EtpiminH and EtOHpiminH were determined using aqueous potentiometric titrations. Solution studies with the ligand piminH were precluded due to the low water solubility of this compound. The stability constants for the VO(IV)–EtpiminH and EtOHpiminH systems were determined and are summarized in Table 3.

The first binding constants could be calculated with a 1:1 metal-to-ligand ratio and precipitation due to the formation of hydrolysis products was observed for titrations with a 1:2 metal-to-ligand ratio. The best fitting experimental curves were obtained using a high metal-to-ligand ratio (10-fold), allowing for the determination of the second binding constants. The species distribution diagram was generated for the VO-EtpiminH system, using the program HySS [40], by inclusion of protonation, stability and hydrolysis constants (Fig. 5).

Both EtpiminH and EtOHpiminH are basic ligands with p*K* values of 7.52 and 7.33, and 11.26 and 11.09 for the imidazoline nitrogen and phenolate oxygen, respectively. As a consequence of this, hydrolysis of vanadyl occurs at a low pH (3 < pH < 7). As the pH increases, however, complex formation prevents the hydrolysis. Experimental data points up to pH 9 fitted well for the complexation studies, and the binary hydroxyl species $[(VO)_2(OH)_5]^-$ and $[VO(OH)_3]^-$ did not fit within the model for highly basic solutions. This is probably due to the high ligand excess and the high thermodynamic stabilization of the vanadium complexes in this pH range due to the basic nature of the ligands. The overall stability constants for these VO-ligand systems are high at 17.13(2) and 16.66(3) for VO-EtpiminH and VO-EtOHpiminH systems, respectively. Both show good overall stability, but are however, subject to hydrolysis at acidic pH range due to the basic nature of the ligands which tend to interact with vanadyl at relatively high pH.

Table 3
Protonation (log *K*) and complex formation constants (log β) for VO(IV)-ligand systems at 25 ± 0.1 °C and *I* = 0.10 M (TMACl).

	Reaction	Ligand		
		EtpiminH	EtOHpiminH	Maltol [39]
pK_1	$LH_2^+ \rightleftharpoons H^+ + LH$	7.52(1)	7.33(1)	
pK_2	$LH \rightleftharpoons H^+ + L^-$	11.26(1)	11.09(1)	8.44(2)
Log β_{110}	$VO^{2+} + L^- \rightleftharpoons [VO(L)]^+$	10.73(2)	10.53(2)	8.80(2)
Log β_{120}	$VO^{2+} + 2L^- \rightleftharpoons [VO(L)_2]$	17.13(2)	16.66(3)	16.29(2)

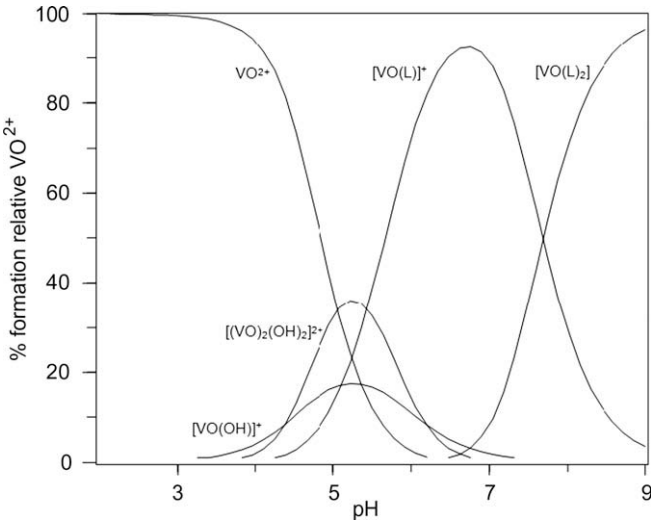

Fig. 5. Species distribution diagram for the complexation of VO(IV) with EtpiminH (LH) [C_{VO} = 0.001 mM and C_L = 0.004 mM].

This hydrolysis could be prevented by encapsulating the complexes within a suitable drug carrier capsule.

3.5. In vitro studies

The vanadium compounds ($VOSO_4$, **1a**, **2** and **3**) showed no cytotoxicity between 0.5 and 10 μM in the 3T3-L1, Chang and C2C12 cell lines tested. At concentrations above 10 μM, however, the vanadium compounds proved to be cytotoxic. Thus, the glucose uptake ability of the vanadium compounds, at non-cytotoxic concentrations of 0.5, 1 and 10 μM, was screened. The results for the 1 μM concentrations are presented in Fig. 5, while the results for all concentrations tested can be found in Table 4.

In the 3T3-L1 adipocytes (Fig. 6), the oxovanadium(IV) compounds ($VOSO_4$, **1a**, **2** and **3**) enhanced glucose uptake significantly, either equaling or surpassing the effects observed for metformin, a drug commonly used in the treatment of type II diabetes [41]. The uptake of glucose in C2C12 muscle cells was not as significant as observed in the other cell lines (Fig. 6). Nevertheless, vanadyl sulfate as well as compounds **1a** and **2** improved glucose uptake relative to the control (Con). The Chang liver cells exhibited the greatest response to the tested compounds compared to the other cell lines tested.

Vanadyl sulfate proved to be the most effective of the oxovanadium(IV) compounds in stimulating the uptake of glucose. This can be attributed to the fact that an *in vitro* model does not take into account that uncomplexed vanadyl ($VOSO_4$) may be simply oxidized to vanadate, the active species for PTP-inhibition, while compounds **1a**–**3** must first undergo oxidation and ligand dissociation. This extra ligand dissociation step may be the reason for the decreased *in vitro* activity of the synthesized compounds [12]. However, the increased stability of compounds **1a**, **2** and **3**, imparted by the organic ligands, may allow vanadium to survive the conditions of the digestive system unlike $VOSO_4$ which undergoes facile hydrolysis and subsequent excretion. It has also been shown that the intestinal cell permeability of complexed vanadium compounds far exceeds that of the inorganic salt ($VOSO_4$) [30]. The effect of the R-substituents (R = H, Et, EtOH) in compounds **1a**–**3** makes little difference to the *in vitro* activity, but would perhaps become important in an *in vivo* model when considering the lipophilicity/hydrophilicity of the complexes. Although the *in vitro* model used may have certain shortcomings, in that it does not

Table 4
The effects of metformin (Met), $VOSO_4$, $[VO(pimin)_2]$ (**1a**), $[VO(Etpimin)_2]$ (**2**) and $[VO(EtOHpimin)_2]$ (**3**) on 3T3-L1, Chang and C2C12 cells at 0.5, 1.0 and 10 μM concentrations. Basal glucose uptake is represented as 100%.

	3T3-L1 adipocytes			Chang hepatocytes			C2C12 myoblasts		
Concentration (μM)									
Compound	0.5	1	10	0.5	1	10	0.5	1	10
Metformin		110 ± 11.1			163 ± 17.2			112 ± 5.3	
$VOSO_4$	123 ± 10.2	126 ± 28.7	129 ± 4.9	131 ± 12.4	154 ± 24.7	122 ± 20.4	235 ± 15.9	111 ± 3.2	50 ± 19.5
$[VO(pimin)_2]$ (**1a**)	122 ± 3.2	120 ± 3.2	121 ± 9.7	109 ± 7.2	141 ± 27.0	116 ± 22.3	88 ± 45.2	107 ± 4.8	87 ± 2.8
$[VO(Etpimin)_2]$ (**2**)	115 ± 11.1	117 ± 0.9	122 ± 20.2	126 ± 26.1	138 ± 32.7	117 ± 31.3	87 ± 4.8	113 ± 31.0	96 ± 8.8
$[VO(EtOHpimin)_2]$ (**3**)	124 ± 4.7	111 ± 11.6	117 ± 3.7	163 ± 7.2	128 ± 31.0	124 ± 31.9	114 ± 8.42	72 ± 3.9	24 ± 3.5

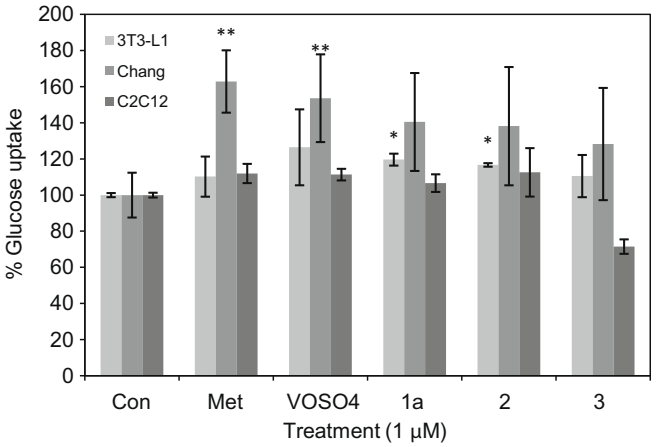

Fig. 6. The effects of metformin (Met), vanadyl sulfate ($VOSO_4$), $[VO(pimin)_2]$ (**1a**), $[VO(Etpimin)_2]$ (**2**) and $[VO(EtOHpimin)_2]$ (**3**) (1 μM) on 3T3-L1, Chang and C2C12 glucose uptake. The basal glucose uptake, is represented as 100% (Con). Error bars indicate SEM ($n = 3$), $^{*}p < 0.05$ and $^{**}p < 0.01$ relative to the (Con).

exactly replicate *in vivo* conditions [42], it does provide a simple and ethical platform for the rapid assessment of new complexes.

4. Conclusions

A series of *bis*[1-*R*-(imidazolinyl)phenolato]oxovanadium(IV) compounds were successfully synthesized and characterized. The compounds **1a**–**3** undergo aerobic oxidation in solution to form the dioxovanadium(V) analogs, one such product (**1b**) was isolated and identified by X-ray crystallography. The acidity constants of EtpiminH and EtOHpiminH, and the stability constants of their corresponding VO(IV) complexes were determined by potentiometric acid–base titrations. These compounds showed encouraging stability and resistance to hydrolysis at relatively high pH, however, modification of the ligands to improve the stability at low pH is currently in progress. The glucose uptake effect of the oxovanadium(IV) compounds was investigated using 3T3-L1 adipocytes, C2C12 muscle cells and Chang liver cells. In the 3T3-L1 adipocytes and Chang liver cells, all of the oxovanadium(IV) compounds (**1a**, **2** and **3**) enhanced glucose uptake, while in the C2C12 muscle cells, all oxovanadium compounds besides **3** showed anti-hyperglycemic activity.

Acknowledgements

The authors thank Dr. E. Antunes from DST/Mintek-NIC (Rhodes University) for the microanalysis results and Mr. T. Mugadza (Rhodes University, Chemistry Department) for assisting with electrochemistry. We acknowledge Miss C. Davison from Nelson Mandela Metropolitan University (Department of Biochemistry and Microbiology) for assisting with the biological assays. For financial support, we thank the South African Medical Research Council (MRC) and National Research Foundation (NRF).

Appendix A. Supplementary material

CCDC 756221 and 756222 contain the supplementary crystallographic data for **1a** and **1b**. These data can be obtained free of charge from The Cambridge Crystallographic Data Centre via www.ccdc.cam.ac.uk/data_request/cif. Supplementary data associated with this article can be found, in the online version, at doi:10.1016/j.ica.2010.03.028.

References

[1] D.O. Abegunde, C.D. Mathers, T. Adam, M. Ortegon, K. Strong, Lancet 370 (2007) 1929.
[2] P. Zimmet, K.G.M.M. Alberti, J. Shaw, Nature 414 (2001) 782.
[3] S. Wild, G. Roglic, A. Green, R. Sicree, H. King, Diabetes Care 27 (2004) 1047.
[4] S. Del Prato, N. Pulizzi, Metabolism 55 (2006) 20.
[5] M. Stumvoll, B.J. Goldstein, T.W. van Haeften, Lancet 365 (2005) 1333.
[6] M.C. Cam, R.A. Pederson, R.W. Brownsey, J.H. McNeill, Diabetologia 36 (1993) 218.
[7] E.H. Clayton, A.G. Tahiliani, J.H. McNeill, Science 227 (1985) 1474.
[8] M.D. Cohen, Toxicol. Ecotoxicol. News 3 (1996) 132.
[9] I.A. Setyawati, K.H. Thompson, V.G. Yuen, Y. Sun, M. Battell, D.M. Lyster, C. Vo, T.J. Ruth, S. Zeisler, J.H. McNeill, C. Orvig, J. Appl. Physiol. 84 (1998) 569.
[10] T. Jakusch, D. Hollender, E.A. Enyedy, C.S. Gonzalez, M. Montes-Bayon, A. Sanz-Medel, J.C. Pessoa, I. Tomaz, T. Kiss, Dalton Trans. (2009) 2428.
[11] D. Sanna, E. Garribba, G. Micera, J. Inorg. Biochem. 103 (2009) 648.
[12] K.G. Peters, M.G. Davis, B.W. Howard, M. Pokross, V. Rastogi, C. Diven, K.D. Greis, E. Eby-Wilkens, M. Maier, A. Evdokimov, S. Soper, F. Genbauffe, J. Inorg. Biochem. 96 (2003) 321.
[13] H. Sakurai, K. Fujii, H. Watanabe, H. Tamura, Biochem. Biophys. Res. Commun. 214 (1995) 1095.
[14] K.H. Thompson, J. Lichter, C. LeBel, M.C. Scaife, J.H. McNeill, C. Orvig, J. Inorg. Biochem. 103 (2009) 554.
[15] T.L. Berridge, J.C. Doxey, A.G. Roach, Eur. J. Pharmacol. 213 (1992) 213.
[16] P. Proks, I. Treinies, H.–J. Mest, S. Trapp, Eur. J. Pharmacol. 452 (2002) 11.
[17] G. Gran, Analyst 77 (1952) 661.
[18] P. Gans, B. O'Sullivan, Talanta 51 (2000) 33.
[19] C. Bazzicalupi, A. Bencini, A. Bianchi, A. Danesi, C. Giorgi, B. Valtancoli, Inorg. Chem. 48 (2009) 2391.
[20] R.P. Henry, P.C.H. Mitchell, J.E.J. Prue, J. Am. Chem. Soc., Dalton Trans. (1973) 1156.
[21] P. Gans, A. Sabatini, A. Vacca, Talanta 43 (1996) 1739.
[22] Bruker, APEX2. Version 2.0-1, Bruker AXS Inc., Madison, Wisconsin, USA, 2005.
[23] Bruker, SAINT-NT. Version 6.0. (includes XPREP and SADABS), Bruker AXS Inc., Madison, Wisconsin, USA, 2005.
[24] Bruker, SHELXTL. Version 5.1. (includes XS, X., XP, XSHELL), Bruker AXS Inc., Madison, Wisconsin, USA, 1999.
[25] A.L. Spek, J. Appl. Crystallogr. 36 (2003) 7.
[26] L.J. Farrugia, J. Appl. Crystallogr. 30 (1997) 565.
[27] T. Mossman, J. Immunol. Met. 65 (1983) 55.
[28] A.S. Keston, in: 129th Meeting American Chemistry Society, 1956, p. 31c.
[29] P. Parík, S. Senauerová, V. Lisková, K. Handlír, M. Ludwig, J. Heterocycl. Chem. 43 (2006) 835.
[30] K.H. Thompson, B.D. Liboiron, Y. Sun, K.D.D. Bellman, I.A. Setyawati, B.O. Patrick, V. Karunaratne, G. Rawji, J. Wheeler, K. Sutton, S. Bhanot, C. Cassidy, J.H. McNeill, V.G. Yuen, C. Orvig, J. Biol. Inorg. Chem. 8 (2003) 66.
[31] A.D. Westland, M.T.H. Tarafder, Inorg. Chem. 20 (1981) 3992.
[32] S. Bhattacharya, T. Ghosh, Trans. Met. Chem. 27 (2002) 89.
[33] G. Wilkinson, R.D. Gillard, J.A. McCleverty, Comprehensive Coordination Chemistry, Elsevier, Pergamon Press, New York, 1987.

[34] A.G.J. Ligtenbarg, A.L. Spek, R. Hage, B.L. Feringa, J. Am. Chem. Soc., Dalton Trans. (1999) 659.
[35] J. Selbin, Chem. Rev. 65 (1965) 153.
[36] C. Bolm, T.K.K. Luongb, K. Harms, Chem. Ber. 130 (1997) 887.
[37] M. Melchior, K.H. Thompson, J.M. Jong, S.J. Rettig, E. Shuter, V.G. Yuen, Y. Zhou, J.H. McNeill, C. Orvig, Inorg. Chem. 38 (1999) 2288.
[38] A.W. Addison, T.N. Rao, J. Chem. Soc., Dalton Trans. (1984) 1349.
[39] K. Saatchi, K.H. Thompson, B.O. Patrick, M. Pink, V.G. Yuen, J.H. McNeill, C. Orvig, Inorg. Chem. 44 (2005) 2689.
[40] L. Alderighi, P. Gans, A. Ienco, D. Peters, A. Sabatini, A. Vacca, Coord. Chem. Rev. 184 (1999) 311.
[41] M.B. Davidson, A.L. Peters, Am. J. Med. 102 (1997) 99.
[42] A.A. Nejo, G.A. Kolawole, A.R. Opuka, J. Wolowska, P. O'Brien, Inorg. Chim. Acta 362 (2009) 3993.